2011

Structural correlates of cytoplasmic and chloroplast lipid body synthesis in Chlamydomonas reinhardtii and stimulation of lipid body production with acetate boost

Carrie Goodson
Washington University in St Louis

Robyn Roth
Washington University School of Medicine in St. Louis

Zi Teng Wang
Washington University in St Louis

Ursula Goodenough
Washington University in St Louis

Eukaryotic Cell

Structural Correlates of Cytoplasmic and Chloroplast Lipid Body Synthesis in Chlamydomonas reinhardtii and Stimulation of Lipid Body Production with Acetate Boost

Carrie Goodson, Robyn Roth, Zi Teng Wang and Ursula Goodenough

Eukaryotic Cell **2011, 10(12):1592. DOI: 10.1128/EC.05242-11.**
Published Ahead of Print 28 October 2011.

EUKARYOTIC CELL, Dec. 2011, p. 1592–1606 Vol. 10, No. 12
1535-9778/11/$12.00 doi:10.1128/EC.05242-11

Structural Correlates of Cytoplasmic and Chloroplast Lipid Body Synthesis in *Chlamydomonas reinhardtii* and Stimulation of Lipid Body Production with Acetate Boost▽†

Carrie Goodson,[1]‡ Robyn Roth,[2]‡ Zi Teng Wang,[1] and Ursula Goodenough[1]*

Department of Biology, Washington University, St. Louis, Missouri 63130,[1] and Department of Cell Biology, Washington University School of Medicine, St. Louis, Missouri 63110[2]

Received 19 September 2011/Accepted 19 October 2011

Light microscopy and deep-etch electron microscopy were used to visualize triacylglyceride (TAG)-filled lipid bodies (LBs) of the green eukaryotic soil alga *Chlamydomonas reinhardtii*, a model organism for biodiesel production. Cells growing in nitrogen-replete media contain small cytoplasmic lipid bodies (α-cyto-LBs) and small chloroplast plastoglobules. When starved for N, β-cyto-LB formation is massively stimulated. β-Cyto-LBs are intimately associated with both the endoplasmic reticulum membrane and the outer membrane of the chloroplast envelope, suggesting a model for the active participation of both organelles in β-cyto-LB biosynthesis and packaging. When *sta6* mutant cells, blocked in starch biosynthesis, are N starved, they produce β-cyto-LBs and also chloroplast LBs (cpst-LBs) that are at least 10 times larger than plastoglobules and eventually engorge the chloroplast stroma. Production of β-cyto-LBs and cpst-LBs under the conditions we used is dependent on exogenous 20 mM acetate. We propose that the greater TAG yields reported for N-starved *sta6* cells can be attributed to the strain's ability to produce cpst-LBs, a capacity that is lost when the mutant is complemented by a *STA6* transgene. Provision of a 20 mM acetate "boost" during N starvation generates *sta6* cells that become so engorged with LBs—at the expense of cytoplasm and most organelles—that they float on water even when centrifuged. This property could be a desirable feature for algal harvesting during biodiesel production.

There is currently keen interest in cultivating eukaryotic algae as sources of triacylglycerides (TAGs) to be converted into diesel and jet transportation fuel (16, 37, 43, 50). In the past 2 years, several laboratories, including ours, have reported that the unicellular green soil alga *Chlamydomonas reinhardtii*, in response to nitrogen (N) starvation, produces TAG-filled lipid bodies (LBs) (9, 21, 23, 24, 30, 31, 44, 49, 51), also called lipid droplets, oil droplets, and oil bodies. Since *C. reinhardtii* currently boasts the best-developed resources for algal molecular-genetic analysis and manipulation (14), it could serve as an important model organism for algal biodiesel research even if it eventually proves to be unsuitable as a production strain.

The structural correlates of LB formation are poorly detailed in algae, in part because algal morphology tends to be poorly preserved when chemical fixatives are used. We therefore undertook an analysis of LB formation in *C. reinhardtii* using phase-contrast and bright-field light microscopy of living cells and deep-etch electron microscopy (DEEM) of quick-frozen living cells. We compared starch-forming strains, primarily a *cw15* strain (herein designated the *STA6* strain), with the *sta6* strain, a starch-null mutant strain derived from the *STA6* strain that has been shown to produce more LBs and TAG than starch-forming strains in several studies (23, 49, 51). We analyzed cells in log and stationary phases, in various stages of N starvation both in liquid medium and on agar plates, and in maturing zygotes. We also assessed the influence of exogenous acetate on LB formation. Results of ongoing collaborations to analyze TAG and gene expression profiles under these various conditions will be reported in separate communications.

Our microscopic findings include the following.

(i) Starch-forming and starchless cells growing in N-replete medium contain occasional small LBs in the cytoplasm (α-cyto-LBs) and occasional small plastoglobules in the chloroplast stroma that make punctate contact with thylakoids.

(ii) N-starved starch-forming cells greatly augment starch biosynthesis and β-cyto-LB production; β-cyto-LBs are intimately associated with both the outer membrane of the chloroplast envelope and the endoplasmic reticulum.

(iii) N-starved starchless cells augment β-cyto-LB production in the same fashion as starch-forming strains. In addition, they produce chloroplast LBs (cpst-LBs) that are far larger than plastoglobules and are commonly enclosed within one or more thylakoids.

(iv) Formation of both β-cyto-LBs and cpst-LBs is dependent on exogenous acetate.

(v) When given a 20 mM acetate "boost" after 2 days of N starvation, both the *STA6* strain and the *sta6* strain continue to augment their LB content until, after 7 to 9 days, they are filled with LBs at the expense of cytoplasmic organelles, notably the chloroplast, a condition we term "obese." Obese starchless cells float on water.

MATERIALS AND METHODS

Strains and culture conditions. Most experiments were conducted with the non-arginine-requiring *cw15* strain CC-4349, described in reference 49, and the

* Corresponding author. Mailing address: Department of Biology, Washington University, 1 Brookings Dr., Campus Box 1229, St. Louis, MO 63130. Phone: (314) 935-6836. Fax: (314) 935-5125. E-mail: goodenough@wustl.edu.

† Supplemental material for this article may be found at http://ec.asm.org/.

‡ C.G. and R.R. contributed equally to this work.

▽ Published ahead of print on 28 October 2011.

cw15 sta6 strain CC-4348 (Chlamydomonas Center), derived from the *cw15* strain. For clarity, these strains are designated the *STA6* strain and the *sta6* strain in this report to emphasize that their key difference lies in their ability versus inability to synthesize starch. Wild-type (wt) *C. reinhardtii* has cell walls and flagella; the *STA6* strain lacks both flagella and cell walls but engages in normal starch biosynthesis, while the *sta6* strain, derived from the parental *STA6* strain by insertional mutagenesis, is wall-less and flagellumless, carries a deletion of the *STA6* gene (which encodes the small subunit of ADP-glucose pyrophosphorylase [53]), and synthesizes no detectable starch (references 23 and 51 and our microscopic observations presented here). Complemented *sta6* strains C2, C4, and C6 were kindly provided by David Dauvillée and Steven Ball (CNRS, Villeneuve d'Asq, France). Zygotes were the products of matings between wt CC-125 and CC-621.

Liquid cultures (75 ml in 150-ml Erlenmeyer flasks) were grown in phosphate-buffered high-salt medium (HSM) (45) containing 9.3 mM NH_4Cl as a nitrogen source and supplemented with 20 mM potassium acetate. Flasks were rotated at 125 rpm under continuous 30-μE illumination from five 20-W daylight fluorescent bulbs (GE F20T12/D). Plate-grown cells were maintained for 30 days on TAP (13) medium supplemented with 1.5% agar (Fluka). Zygotes were matured on N-free TAP plates. Cultures were inoculated from plates and grown to log phase (mean hemacytometer count of 48 cultures, $2.6 \times 10^6 \pm 1.2 \times 10^6$ cells/ml), pelleted at $800 \times g$, and resuspended in 75 ml HSM containing 20 mM acetate and lacking NH_4Cl. In some experiments, 1 ml of 1.5 M potassium acetate was added to cultures that had been N starved for 2 days (the 20 mM acetate boost). The pH of a freshly inoculated HSM+acetate culture is 7.0; during 5 days of N starvation with an acetate boost, the pH of the culture increases to 8 to 8.5.

Microscopy. For light microscopy, 750 μl of cell culture was pelleted at $800 \times g$ and brought up in 15 μl of its own supernatant to generate dense fields of cells for photography (a procedure not possible for obese cells; hence, their images are more dispersed). Cells were examined and photographed using a Wild M20 phase-contrast bright-field microscope with a 40× objective, a 1.25× Variomag, and a 2.5× camera adapter (Canon EOS Rebel XTi). All fields were photographed at the same magnification. Calculations of numbers of LBs/cell (see Fig. 6) were made using micrographs of "popped" cells or intact cells that were sufficiently dry that their LB content could be readily scored. More than 2,000 light micrographs from 72 independent samples were examined for this study.

For electron microscopy, live cells were pelleted at $800 \times g$ or scraped from agar plates. Obese cells were recovered from the meniscus after centrifugation. Cells were layered onto cushioning material, dropped onto the surface of a helium-cooled copper block, fractured, etched, and rotary replicated with platinum and carbon using the protocols and apparatus developed by Heuser (15). More than 2,000 DEEM micrographs from 48 independent samples were examined for this study.

RESULTS

Light microscopy. Figures 1 to 5 present montages of living *STA6* and *sta6* cells visualized by phase-contrast and bright-field (Fig. 4) microscopy, all photographed and printed at the same magnification; additional images are presented in File 1 in the supplemental material. The immotile cells settle onto the glass slide without fixation, and since they lack cell walls, they flatten out as they dry, permitting high-resolution images. Eventually they "pop" when the plasma membrane lyses (49), depositing their starch and LBs (the *STA6* strain) or their LBs (the *sta6* strain) *in situ* on the slide. The two contractile vacuoles continue to pump until a cell pops, indicating that the cells are still operant during the drying process.

(i) N starvation for 2 days from log phase. Figure 1A shows *sta6* cells in mid-log phase (2×10^6 to 3×10^6 cells/ml); Fig. 1B and C show *sta6* cells after 1 and 2 days of N starvation from log phase in 20 mM acetate. The range in cell size reflects different stages of the cell cycle. Cell numbers in cultures increase after transfer to N-free medium (27), stabilizing at 0.8×10^7 to 1×10^7 after 1 day.

Round luminous LBs are just visible in 1-day N-starved *sta6* cells (Fig. 1B) and conspicuous in 2-day N-starved *sta6* cells

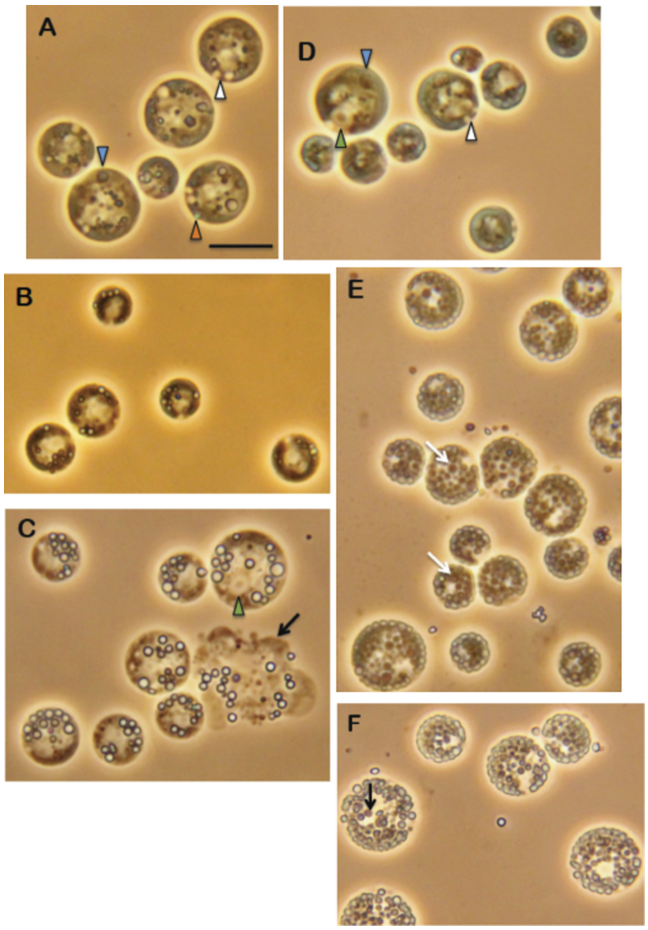

FIG. 1. Cells in N-replete medium and cells that were N starved up to 2 days (additional images are presented in File 1 in the supplemental material). Green arrowheads, nuclei with central nucleoli; white arrowheads, contractile vacuoles; orange arrowheads, eyespots (which refract blue with phase optics); blue arrowheads, pyrenoids. (A) *sta6* cells in log phase. Internal refractile bodies are polyphosphate granules of acidocalcisomes (8, 39). (B) *sta6* cells that were N starved for 1 day. Round white inclusions are LBs. (C) *sta6* cells that were N starved for 2 days; a popped cell (49) is indicated by an arrow (File 2 in the supplemental material shows the popping process for this field of cells). (D) Log-phase *STA6* cells. (E) *STA6* cells that were N starved for 2 days. Starch appears white at the cell periphery and brown in the interior. Arrows indicate interior LBs. (F) *sta6* cells complemented with a *STA6* transgene. Starch is white at the periphery and brown in the interior (arrow). All micrographs are at the same magnification; bar, 10 μm.

(Fig. 1C). Included in Fig. 1C (arrow) is a popped cell (49) displaying its LB content. A time course of popping cells, found in File 2 in the supplemental material, illustrates several important features of the popping process: when the cell membrane lyses, the LBs neither fragment nor fuse, nor do they change in size when they adsorb to the glass slide.

STA6 cells make little starch during growth (Fig. 1D), but during the first 2 days of N starvation they produce abundant starch (44, 49, 51), visible in Fig. 1E as a rim of refractile granules around each cell perimeter and as brown clumped material in the cell interior. Larger brown spherical LBs are also evident in the cell interior (Fig. 1E, arrows). When the

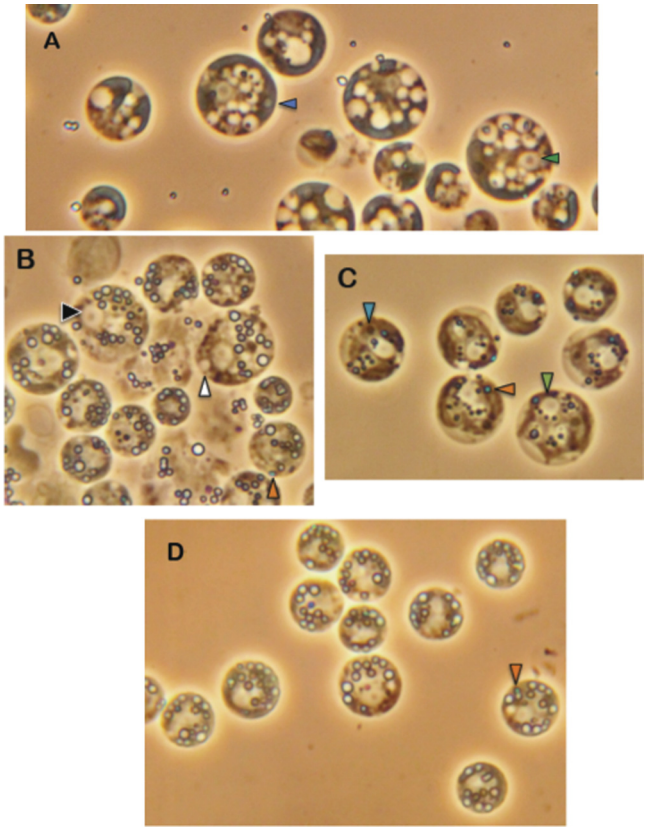

FIG. 2. *sta6* cells in various growth or induction conditions (additional images are presented in File 1 in the supplemental material; symbols are as in Fig. 1). (A) *sta6* cells in stationary phase. Vacuoles in interior often contain polyphosphate granules. (B) *sta6* cells that were N starved from stationary phase for 2 days. The field includes many lysed cells. (C) *sta6* cells that were N starved from log phase for 2 days without acetate. Cells contain polyphosphate granules but no detectable LBs. (D) *sta6* cells grown in minimal (no acetate) medium and then N starved from log phase for 2 days with 20 mM acetate. The magnification is the same as in Fig. 1.

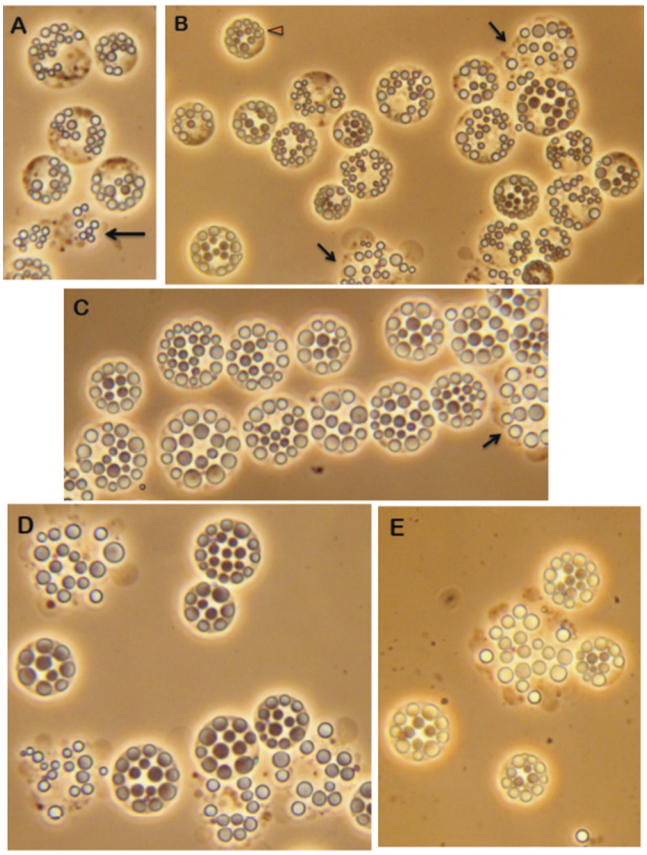

FIG. 3. *sta6* cells that were N starved for 4 or more days with and without acetate boost (additional images are presented in File 1 in the supplemental material). *sta6* cells were N starved for 4 days without acetate boost (A) or N starved with an acetate boost for 4 days (B), 6 days (C), 8 days (D; note the four popped cells), or 10 days (E; note the popped cell). Arrows indicate popped cells. The magnification is the same as in Fig. 1.

sta6 strain is complemented with a *STA6* transgene and N starved for 2 days, the cells display the *STA6* phenotype (Fig. 1F), with abundant starch and interior LBs (arrow). Because starch accumulation obscures LB profiles, most of the light-microscope images in this report show *sta6* cells.

(ii) N starvation of cells from log versus stationary phase. In our previous study (49), cells were N starved after entering stationary phase ($\sim 1 \times 10^7$ to 2×10^7 cells/ml). As will be described in detail elsewhere (R. Roth and U. Goodenough, unpublished data), *STA6* and *sta6* cells undergo an extensive autophagocytic program when they enter stationary phase, observable in Fig. 2A as large populations of cytoplasmic vacuoles containing polyphosphate granules (derived from organelles called acidocalcisomes [8, 39]). Stationary-phase cells produced smaller LBs after 2 days of N starvation than log-phase cells (compare Fig. 1C and 2B); moreover, they became moribund and tended to lyse after 2 days (Fig. 2B). Therefore, most of the images in this report depict cells that were N-starved from log phase.

(iii) N starvation of cells without acetate. Figure 2C shows *sta6* cells that were N starved in the light for 2 days without acetate. The omission of acetate prevents the accumulation of any visible LBs in both the *sta6* strain and the *STA6* strain, although there is no inhibitory effect on starch accumulation (27). When the acetate-free cells are provided with 20 mM acetate after 2 days, they engage in robust LB formation during the following 2 days (see File 3 in the supplemental material).

(iv) N starvation of cultures grown in the absence of acetate. While both strains require exogenous acetate for N-stress-induced LB formation under the conditions employed, it is not necessary that the cells be cultivated in the presence of acetate. Figure 2D shows *sta6* cells that were grown in the light in acetate-free HSM and then transferred in log phase to acetate-containing N-free HSM for 2 days. LB levels are comparable to those in cells that were grown in acetate-containing medium (Fig. 1C).

(v) Long-term maintenance of N-starved *sta6* cells and effects of an acetate boost. Figure 3A shows *sta6* cells N starved in acetate from log phase for 4 days. LB size clearly increased compared with that in 2-day cells (Fig. 1C), but when such cells were incubated for more than 4 days, they became moribund and lysed.

However, when *sta6* cells were given an additional 20 mM

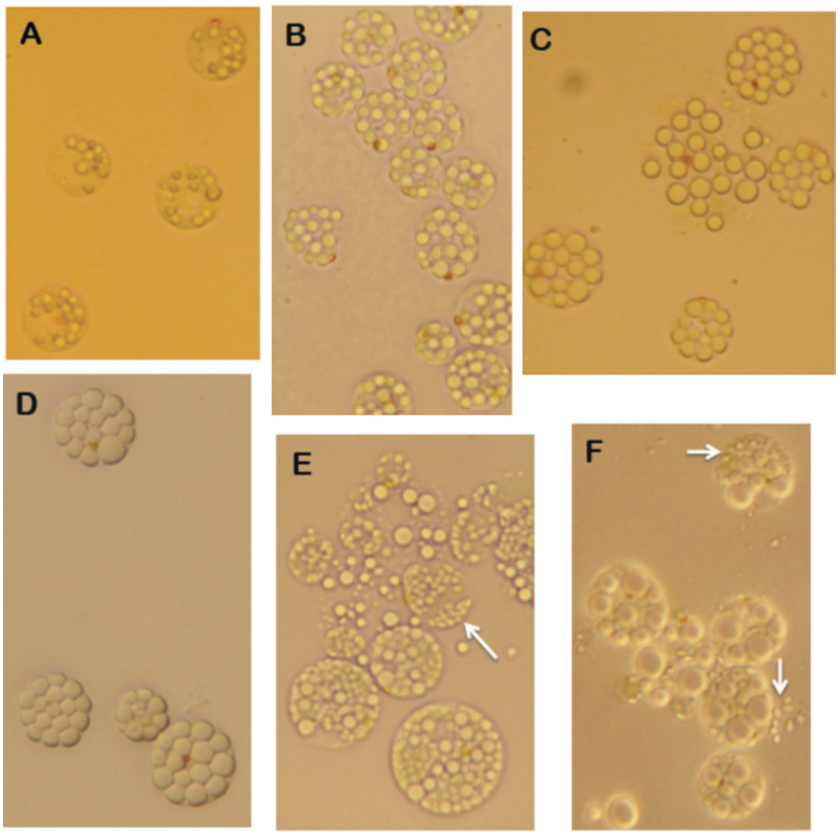

FIG. 4. Bright-field images of N-starved cells (additional images are presented in File 1 in the supplemental material). Eyespots are orange. *sta6* cells were N starved for 2 days (A) or N starved with an acetate boost for 4 days (B), 10 days (C; note the popped cell), or 14 days (D). *STA6* cells were N starved for 4 (E) or 14 (F) days with an acetate boost. Arrows indicate starch. The magnification is the same as in Fig. 1.

acetate (from a concentrated stock) after a 2-day N starvation in 20 mM acetate, they remained viable up to 2 weeks, and their LBs continued to enlarge. An acetate boost also enhanced the LB size of *sta6* cells first grown to log phase in minimal medium (see File 3 in the supplemental material).

Figure 3B to E show N-starved acetate-boosted *sta6* cells after 4, 6, 8, and 10 days of culture. The LBs greatly increased in size with continued incubation. This is also evident in popped-cell fields (a gallery of popped-cell images is found in File 4 in the supplemental material) and in bright-field images (Fig. 4A to D), where LBs increasingly fill the cells until they appear "stuffed." We designate such cells as obese.

When observed by phase-contrast microscopy, the LBs of obese *sta6* cells are lighter in color at the cell perimeter than in the interior (Fig. 3). As documented with DEEM (see below), the LBs at the perimeter are located in the peripheral chloroplast (cpst-LBs), while those in the interior are located in the cytoplasm (β-cyto-LBs). The color differential is lost when the *sta6* cells pop (Fig. 3D and E), indicating that it is a phase-optics effect.

Beginning at 5 days after N starvation, obese *sta6* cells became sufficiently lipid filled that they tended to float up to the meniscus of a culture tube, and they collected at the meniscus when a culture aliquot was centrifuged at 800 × *g*, 16,000 × *g*, or 100,000 × *g* (cells normally pellet at 800 × *g*). Full "floatability" was displayed by boosted *sta6* cultures after 7 to 9 days.

Obese *sta6* cultures became increasingly yellow with long-term culture, during which time their thylakoids were all but eliminated (see below). Although the LBs continued to increase in size, cell size itself remained fairly constant, since the cells were losing both chloroplast and cytoplasmic volume (see below). When aliquots of yellow cultures were inoculated into N-replete medium, at least some of the cells remained viable (quantitative analyses of viability are in progress). The culture turned white when the cells died (typically after 2 weeks), at which time the cells lysed and the LBs tended to clump.

(vi) Long-term maintenance of N-starved *STA6* cells and effects of acetate boost. As documented with DEEM (see below), the *STA6* strain did not make cpst-LBs, producing LBs only in the cytoplasm. After 4 days of N starvation, these LBs appeared as brown internal spheres (white arrows in Fig. 5A) surrounded by a rim of white refractile starch, and they were visibly larger than in the 2-day sample (Fig. 1E).

When given an acetate boost after 2 days of N starvation, *STA6* cells at 4 days displayed two differences from nonboosted cells (compare Fig. 5A and B): the LBs in the boosted cells were somewhat larger, and some were located at the periphery and hence appeared lighter (white arrows in Fig. 5B). These trends continued with longer incubations: at 9 days (Fig. 5C) and 14 days (Fig. 5D), the LBs were greatly enlarged, and many had the light color imparted by a peripheral location.

Accompanying the increase in LB size and change in distri-

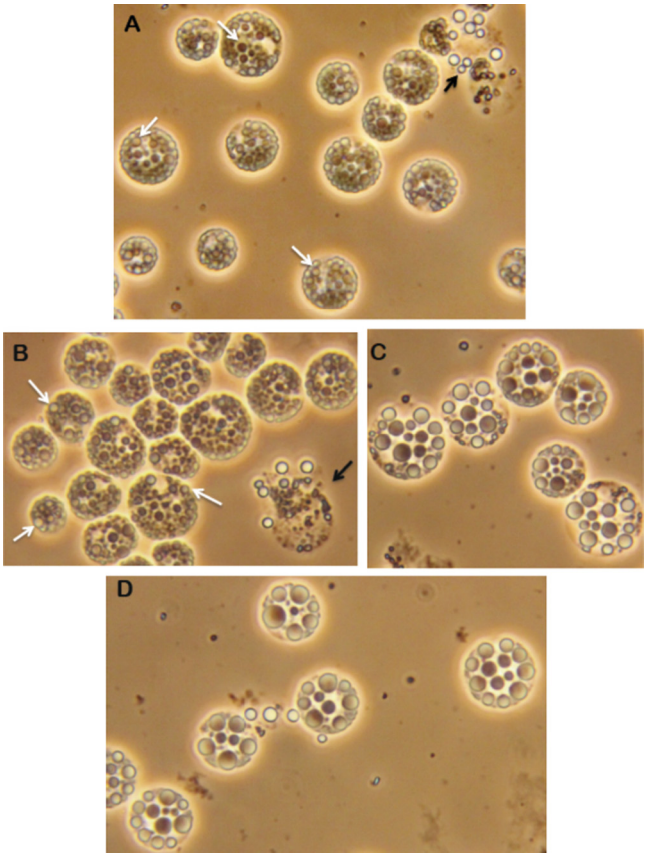

FIG. 5. *STA6* cells that were N starved for 4 or more days with and without acetate boost (additional images are presented in File 1 in the supplemental material). (A) *STA6* cells that were N starved for 4 days without acetate boost. Starch appears white at the cell periphery and brown in the interior (white arrows). Black arrow, popped cell. (B) *STA6* cells that were N starved for 4 days with an acetate boost. White arrows, interior LBs; black arrow, popped cell. (C) *STA6* cells that were N starved for 9 days with an acetate boost. (D) *STA6* cells that were N starved for 14 days with an acetate boost. The magnification is the same as in Fig. 1.

bution, boosted *STA6* cells depleted their starch reserves with incubation time. This is most readily seen with bright-field microscopy, where the refractile starch is easily identified. Figure 4E and F contrast 4-day-boosted with 14-day-boosted *STA6* cells, where the decrease in starch levels (white arrows) and the increase in LB size are evident. Despite this loss of starch, obese *STA6* cells did not display the floatability of obese *sta6* cells, presumably because some starch remained (starch is very dense, 1,500 kg/m^3 [46]). Hence, the majority of *STA6* cells continued to pellet at 800 × *g* up to 14 days.

Obese *STA6* cultures turn yellow and die more slowly than *sta6* cultures, and the cells retain more cytoplasm (see below), possibly because the cells are provided with starch reserves.

(vii) Lipid bodies per cell. In a previous study (49) we quantitated the area of Nile red-stained LBs to obtain an estimate of LB yield. Since area increases as a function of the square of the radius (r^2), whereas volume increases as a function of r^3, area measurements become increasingly uninformative when LB volume increases, as occurs during the long-term studies reported here. TAG yield is therefore being evaluated with biochemist collaborators and will be reported elsewhere.

Meanwhile, the light-microscopy images obtained in the current study are well suited to evaluation of the number of LBs per cell, regardless of size, under various induction conditions. Figure 6 plots these findings. The *STA6* strain maintained a narrow range of numbers of LBs/cell (4 to 12) during the first 96 h, while the median increased somewhat with extended culture. The *sta6* strain had 1.5 to 2 times more LBs/cell than the *STA6* strain at each time point, presumably due to its cpst-LB population, and the range (6 to 25 LBs/cell) was considerably larger, but the median held steady at 12 to 15 LBs/cell. While not evaluated at all time points, *sta6* cells complemented with *STA6* transgenes showed an LB/cell distribution identical to that of the *STA6* strain after 48 h N starvation, with a range of 4 to 12, a mean of 7.2, and a median of 7 (n = 22).

Deep-etch electron microscopy. Pellets of live cells were quick-frozen at liquid-helium temperatures, fractured, deep-etched, and replicated using Pt/C rotary-shadowing (15). Cellular inclusions containing neutral lipid are unmistakable in such replicas: the fracture plane travels through their interior to create a blunt, smooth, featureless domain, much like a pat of butter. Additional DEEM figures are presented in File 5 in the supplemental material.

(i) Neutral-lipid-containing inclusions in N-replete log-phase cells. When N-replete *C. reinhardtii* cells are solvent extracted and analyzed biochemically, low levels of TAG are detected (23, 31, 44), as are low levels of Nile red-fluorescent bodies (49, 51). DEEM identifies three morphological correlates of this "constitutive TAG": eyespot granules and plastoglobules in the chloroplast and α-cyto-LBs in the cytoplasm.

(a) Eyespot granules. Eyespot granules (Fig. 7A), 75 to 100 nm in diameter, associate to form an opaque shield behind a circular photosensitive patch of the plasma membrane (20). They contain orange carotenoids (Fig. 4), and the TAG profile of purified eyespots has been characterized (31). The granules tend to be hexagonal (Fig. 7A), suggesting that the fibrillin proteins in their encapsulating membranes or coats (41) may impose structural constraints.

(b) Plastoglobules. Plastoglobules (Fig. 7B), 50 to 150 nm in diameter, are round proteo-membrane-limited inclusions that are ubiquitous in land plant chloroplasts (5, 18). Presumed homologous inclusions have been observed in the stroma of certain algae (reviewed in reference 20) and are evident in EM studies of *C. reinhardtii* from the Palade laboratory (4, 7, 34, 40). They make punctate contacts with thylakoids in the fashion of their land plant counterparts (2). Their TAG content is inferred from their featureless fracture faces and from analyses of land plant plastoglobules (17), but nothing is yet known about their protein content or their TAG profile or about whether they contain pigments.

(c) α-cyto-LBs. α-Cyto-LBs (Fig. 7C and D) presumably correspond to the bodies occasionally visualized by Nile red or Bodipy fluorescence in N-replete cells (49, 51). They are infrequent and small, ranging in size from 250 to 1,000 nm. Most are in contact with the endoplasmic reticulum (ER) and/or nuclear envelope (Fig. 7C), and some make contact as well with mitochondria (Fig. 7D) or acidocalcisomes, but chloroplast contact, when observed, is punctate. α-cyto-LBs often localize between the chloroplast and the plasma membrane

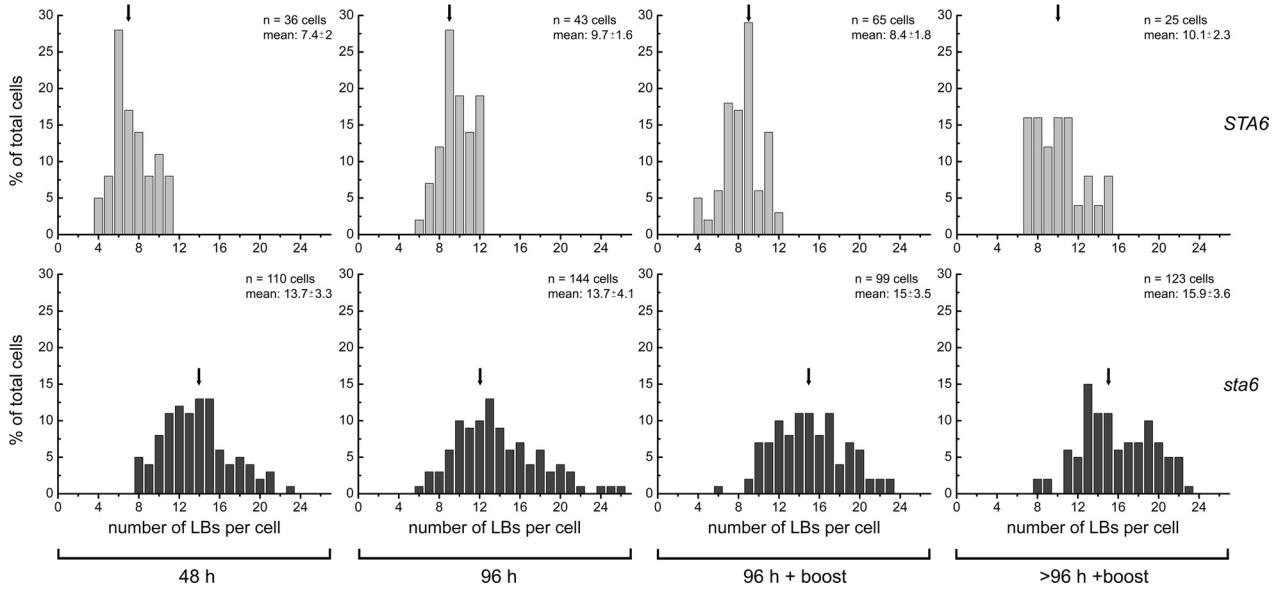

FIG. 6. Number of LBs per cell, expressed as a percentage of the total cells scored in a given sample. Arrows indicate median values. (Top) *STA6* cells that were N starved for 48 h, 96 h, 96 h with an acetate boost, and >96 h with an acetate boost (pooled samples up to 13 days). (Bottom) *sta6* cells that were N starved for 48 h, 96 h, 96 h with an acetate boost, and >96 h with an acetate boost (pooled samples up to 10 days).

(Fig. 7D), a location never observed for the β-cyto-LBs (described below).

(ii) β-Cyto-LBs: general features. β-Cyto-LBs were found only in N-starved cells, first appearing ~15 h after transfer from log-phase growth. They became increasingly enlarged and abundant as N starvation progressed in all strains analyzed (the *STA6*, *sta6*, and complemented *sta6* strains and two wt strains); in parallel, α-cyto-LBs became progressively uncom-

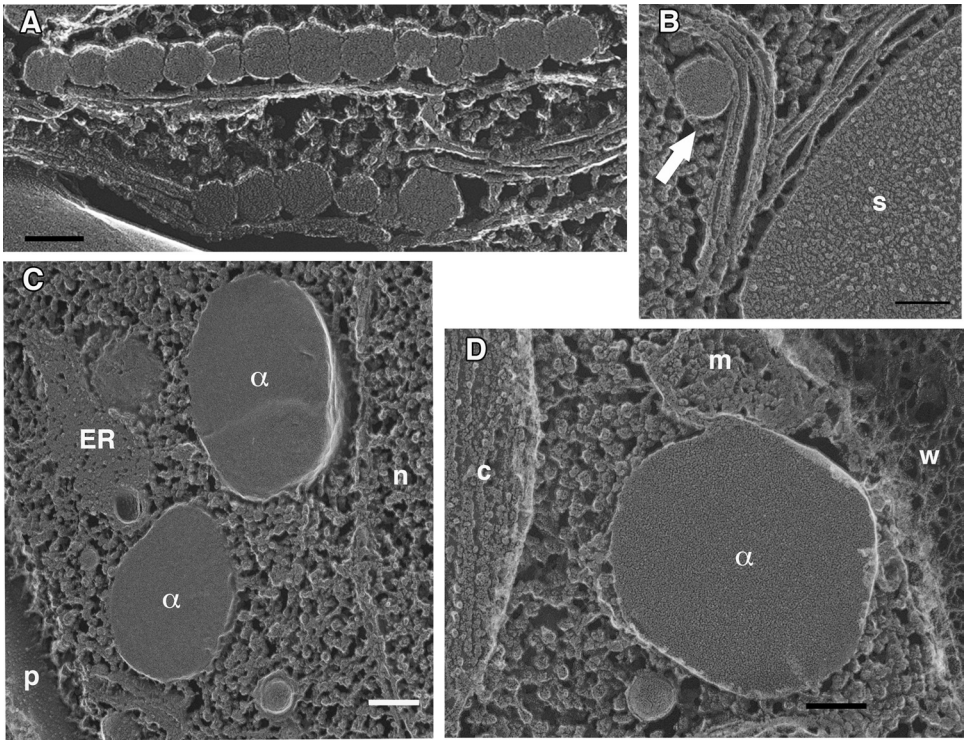

FIG. 7. Constitutive TAG-containing bodies (additional images are presented in File 5 in the supplemental material). Bars, 100 nm. (A) Two rows of eyespot granules in contact with thylakoid membranes. *sta6* cells were N starved for 30 h from stationary phase. (B) Plastoglobule (arrow) in contact with thylakoid membrane. s, starch. *STA6* cells were N starved for 48 h. (C) α-cyto-LBs in contact with or proximate to the ER and nuclear envelope. n, nucleus; p, plasma membrane (wt cells were examined in log phase). (D) α-cyto-LB in contact with a mitochondrion (m). c, chloroplast; w, cell wall fibrils. wt cells were examined in log phase.

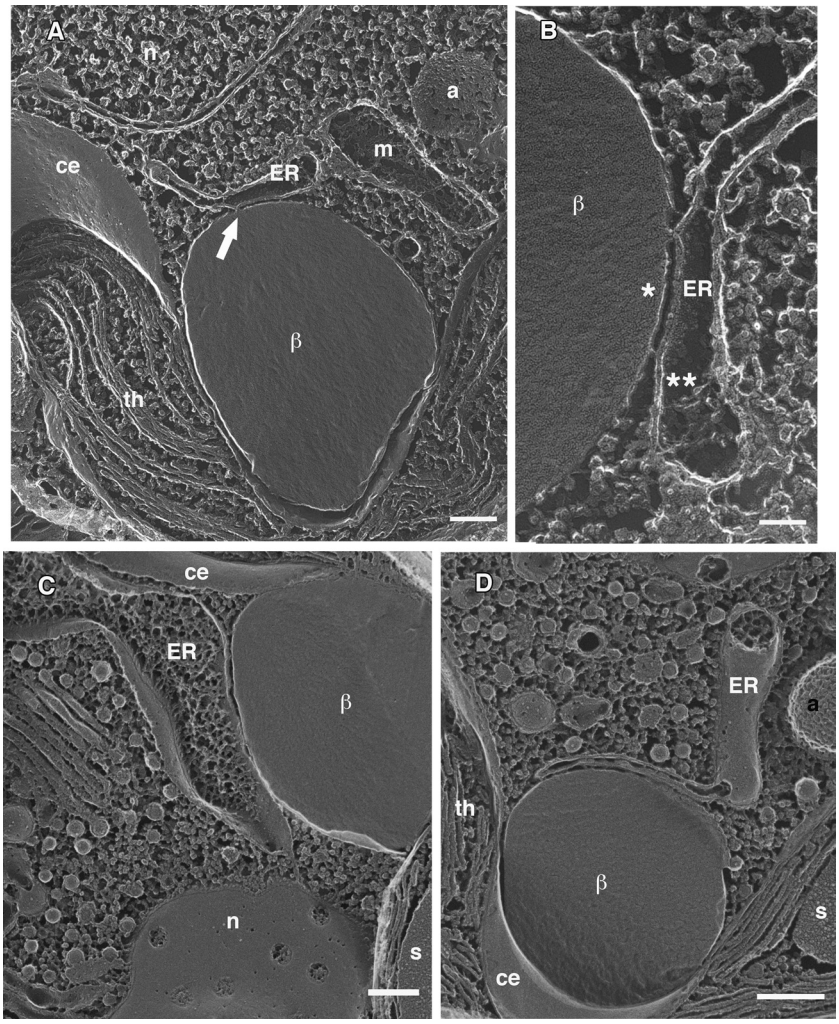

FIG. 8. β-Cyto-LBs and ER (additional images are presented in File 5 in the supplemental material). (A) β-Cyto-LB in contact with an ER element (arrow) and the chloroplast. a, acidocalcisome (8, 39); ce, OMCE; m, mitochondrion; n, nucleus; th, thylakoids. *sta6* cells were N starved for 30 h from stationary phase. Bar, 100 nm. (B) Enlargement of panel A, showing the ER membrane bilayer (double asterisk) and LB monolayer (single asterisk). Bar, 50 nm. (C) β-Cyto-LB in contact with an ER cisterna that is feeding vesicles to the Golgi at middle left; contact with the OMCE (ce) is seen at the top. n, nuclear envelope with pores; s, starch granule. *STA6* cells were N starved for 48 h. Bar, 250 nm. (D) β-Cyto-LB in contact with a narrow ER element branching from a broader cisterna and with the OMCE (ce). a, acidocalcisome; s, starch; th, thylakoids. *STA6* cells were N starved for 48 h. Bar, 250 nm.

mon and were not encountered after 24 h of N starvation, suggesting that they may serve to "seed" the β-cyto-LBs (see below). β-Cyto-LBs were also abundant in developing and mature wt zygotes (see File 6 in the supplemental material). In our previous study (49), β-cyto-LBs from *STA6* and *sta6* cells were purified, and their fatty acid methyl esters (FAMEs) and charged polar lipids were characterized. A fraction enriched in wt β-cyto-LBs was also analyzed biochemically by Moellering and Benning (31).

β-Cyto-LBs invariably localized between the interior surface of the cup-shaped chloroplast and the nucleus (Fig. 8A), and they displayed close relationships with two membrane systems, the ER and the outer membrane of the chloroplast envelope (OMCE). Features of these relationships are shown in Fig. 8 to 10.

(iii) β-Cyto-LB relationships with ER. An element of the ER is almost invariably found in close association with one surface of a β-cyto-LB, a relationship also encountered in land plant seeds (42) and animal cells (11). Some cross-fractures (Fig. 8A, arrow; enlarged in Fig. 8B) provide excellent views of the continuity between the outer leaflet of the ER membrane and the lipid monolayer surrounding the β-cyto-LB, concordant with ER-LB topology in other systems (42). In many cases, the fractures reveal more extensive ER–β-cyto-LB associations, sometimes involving up to half the β-cyto-LB surface, with numerous punctate associations between the enfolding ER bilayer and the β-cyto-LB monolayer. Figure 8C shows a "multitasking" ER cisterna coming off the nuclear envelope, blebbing off vesicles to the Golgi on the left side and making extended contact with a β-cyto-LB on the right side. Figure 8D shows a large ER cisterna giving off a narrow tubular element that makes extended β-cyto-LB contact.

Figure 9A and B show additional features of the LB/ER relationship. In Fig. 9A, an ER membrane displays a signature

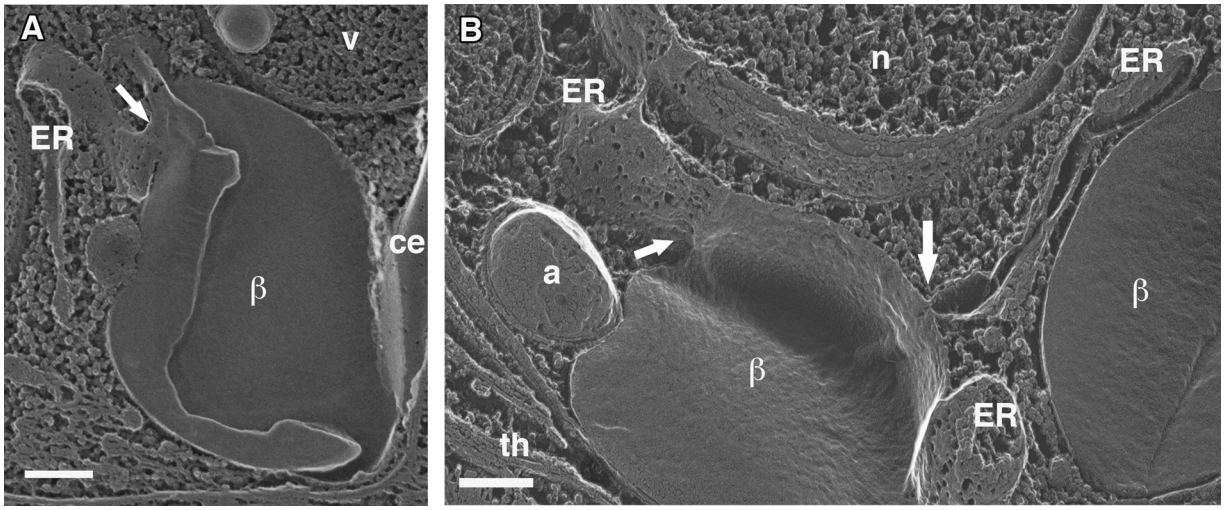

FIG. 9. Membrane relationships between β-cyto-LBs and ER (additional images are presented in File 5 in the supplemental material). (A) β-Cyto-LB associated with an ER cisterna whose membrane flows over the LB surface. The arrow indicates the junction between the intramembranous-particle (IMP)-pit-rich and IMP-free domains. ce, OMCE; v, vacuole. *sta6* cells were N starved for 12 h from stationary phase. Bar, 100 nm. (B) Two β-cyto-LBs, the right fractured through its TAG interior, the left along its surrounding monolayer. Right arrow, ER membranes feeding directly into the IMP-free LB monolayer; left arrow, IMP-pit-rich ER, extending off the nuclear envelope, continuous with the IMP-free LB monolayer. a, acidocalcisome; n, nucleus; th, thylakoids. *sta6* cells were N starved for 30 h from stationary phase. Bar, 250 nm.

array of intramembranous-particle (IMP) pits that form when transmembrane proteins are pulled out of the membrane during fracture. At its junction with an LB (arrow), a naked monolayer spreads over the LB, leaving the IMP pits behind. Figure 9B shows two β-cyto-LBs and two ER cisternae. The cisterna to the right makes lateral contact with the one LB and then feeds directly into the second LB. Such "direct feeds" were visualized ~20 times in the course of this study (additional examples are presented in File 5 in the supplemental material), suggesting that they are rare and/or transient occurrences. The cisterna to the left, coming off the nuclear envelope, makes the same kind of pit/no-pit junction as was noted in Fig. 9A. Such junctions support our earlier finding that purified β-cyto-LBs are devoid of protein (49).

(iv) β-Cyto-LB relationships with the OMCE. The OMCE is almost invariably closely associated with the non-ER-associated surface of a β-cyto-LB (Fig. 8 and 9); indeed, β-cyto LBs typically "snuggle" into infoldings of the chloroplast surface (Fig. 8A, C, and D).

Figure 10A to C show additional features of the β-cyto-LB–OMCE relationship. In Fig. 10A and B, the OMCE, which is virtually IMP free in N-starved cells (cf. Fig. 8A), appears to "flow" over the β-cyto-LB exterior in the manner described above for the flow of the ER membrane (Fig. 9A and B); an interpretation of these configurations is offered in the Discussion. Figure 10C shows these relationships in cross-fracture: a β-cyto-LB is in extensive contact with the nuclear envelope and ER on one face (upper arrow), while a second face makes a long association, with frequent punctate contacts, with the OMCE (left arrow).

(v) Relationship between α-cyto-LBs and β-cyto-LBs. Careful scrutiny of hundreds of DEEM micrographs recording the early hours of N starvation failed to yield examples of small nascent β-cyto-LBs sandwiched between ER and OMCE membranes; instead, when β-cyto-LBs were first encountered, at ~15 h, they were invariably already in the size range of large α-cyto-LBs (Fig. 7D). This observation suggests that in response to N starvation, α-cyto-LBs may seed the formation of β-cyto-LBs, recruiting the stable ER and OMCE associations entailed in the extensive β-cyto-LB enlargement that occurs at later stages.

(vi) Cpst-LBs: general features. In exhaustive analyses of growing and N-starved starch-producing cells in liquid medium, on agar plates sampled over the course of 30 days, and in zygotes, including three starch-producing *sta6* strains complemented by *STA6* transgenes, none was observed to contain cpst-LBs.

In contrast, cpst-LBs are an invariant feature of N-starved *sta6* cells. In a time course DEEM study, cpst-LBs were not detected at 2, 4, or 8 h after *sta6* cells were N starved from log phase, but they were frequently encountered at 12 h, and they increased in size until they dominated the chloroplast stroma. In our previous study (49), cpst-LBs were scored in popped-cell assays of the *sta6* strain, but they did not contribute to our purified *sta6* LB preparations, since the cell breakage procedure employed was designed to leave chloroplasts intact.

Cpst-LBs are shown in Fig. 10A and 11A to C. Each cpst-LB is delimited by a membrane monolayer; examples are indicated with asterisks in Fig. 11A and B. In addition, most are at least partially enveloped by one or more thylakoids, a configuration we designate the "thylakoid wrap." Cross-fractured single wraps are indicated by arrows in Fig. 11A and B. In en face views of wraps (Fig. 10A and 11A and C), the IMP-free thylakoid membrane appears to flow over the cpst-LB surface, reminiscent of ER and OMCE relationships with β-cyto-LBs. Images such as the upper region of Fig. 11C suggest that the thylakoid membrane may also disassemble in conjunction with cpst-LB assembly.

(vii) Relationship between cpst-LBs and plastoglobules. When first encountered in N-starved *sta6* cells, cpst-LBs al-

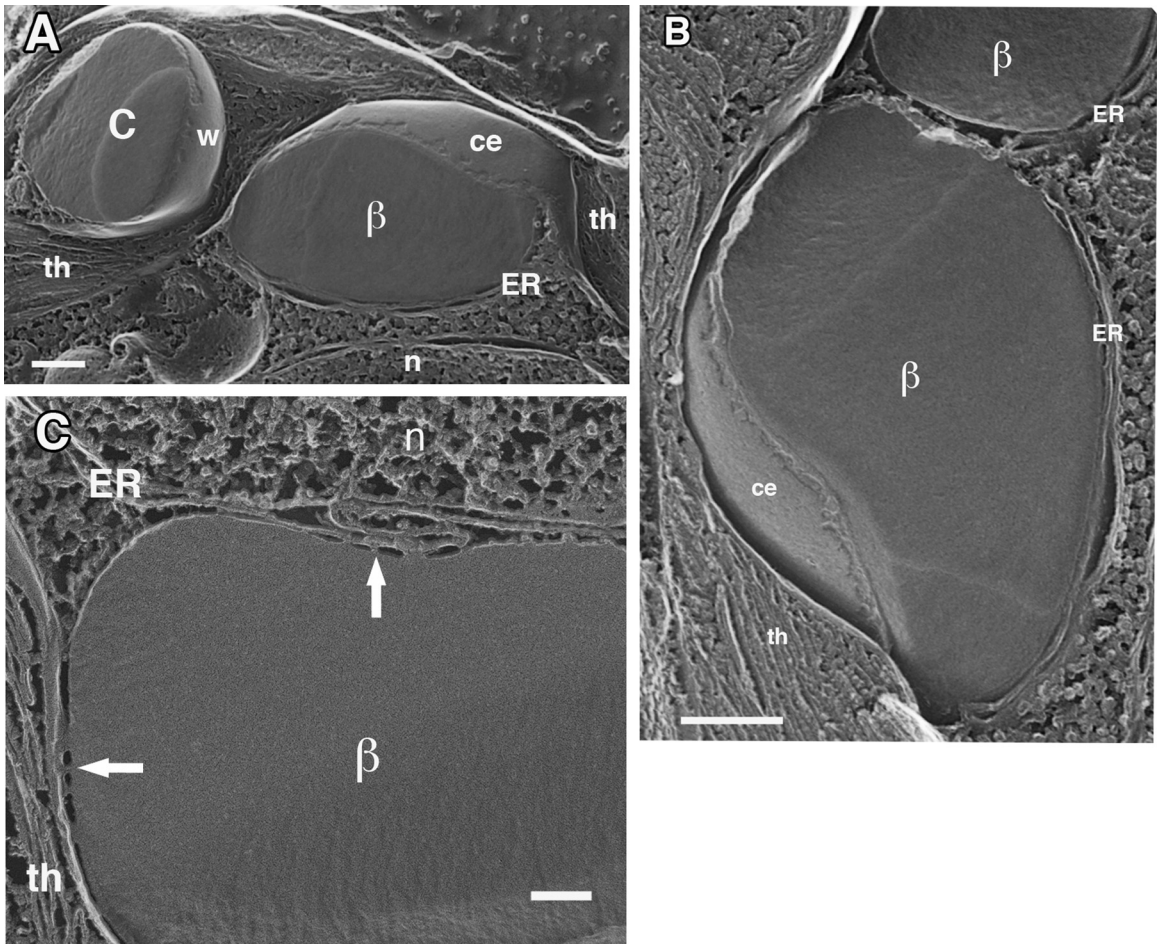

FIG. 10. Membrane relationships between β-Cyto-LBs and OMCE (additional images are presented in File 5 in the supplemental material). (A) β-Cyto-LB with the ER in contact with one face and the OMCE (ce) flowing over the opposite face. Also shown is a chloroplast LB (C) with an IMP-free thylakoid wrap (w) flowing over its surface. n, nucleus; th, thylakoids. *sta6* cells were N starved for 30 h from stationary phase. Bar, 250 nm. (B) Two contiguous β-cyto-LBs associated with ER on one face and OMCE (ce) flowing over the opposite face. th, thylakoids. *sta6* cells were N starved for 30 h from stationary phase. Bar, 250 nm. (C) β-Cyto-LB in contact with the ER and nuclear envelope (upper arrow) and with the OMCE (left arrow). n, nucleus; th, thylakoids. *STA6* cells were N starved for 48 h. Bar,100 nm.

ready measured 0.5 to >1 μm; small nascent cpst-LBs with thylakoid wraps were not observed, although these might be difficult to identify. This is reminiscent of our failure, noted above, to identify nascent β-cyto-LBs. Possibly, therefore, the small plastoglobules in the chloroplast stroma serve to seed cpst-LB formation in the *sta6* strain, with their punctate thylakoid contacts shifting to the more extensive wrapped configurations (see Discussion).

(viii) Fine structure of cells subjected to extended N starvation and acetate boost. After 4 days of N starvation with an acetate boost (see above), the chloroplasts of obese *STA6* cells are starch replete and contain extended thylakoids, and the β-cyto-LBs retain their canonical relationship with the ER and OMCE (Fig. 12A). After 14 days (Fig. 12B), *STA6* chloroplasts are greatly reduced in size but retain some starch, and the remaining thylakoids are extended and display IMPs. While the enormous β-cyto-LBs often extend out to the cell surface, as previously noted by phase microscopy (Fig. 5), their relationship with the ER and OMCE persists.

After 4 days of N starvation with an acetate boost, the thylakoids of obese *sta6* cells lost their extended configuration and were severed into short segments (Fig. 13A), a phenotype that correlates temporally with the onset of yellowing of the culture. After 10 days, the chloroplasts containing severed thylakoids were reduced to small islands (Fig. 13B), and the cellular interior was largely LBs, where it was no longer possible to distinguish cytoplasmic and chloroplast species.

Figure 14 compares a 14-day-boosted *STA6* cell with a 7-day-boosted *sta6* cell, highlighting the extreme obesity achieved by the *sta6* strain in a far shorter period. The only identifiable organelles in such *sta6* cells are the nucleus, the chloroplast envelope (which retains its normal surface area even when devoid of thylakoids), the eyespot (Fig. 4D), and the plasma membrane.

DISCUSSION

Light microscopy and lipid bodies per cell. Light microscopy permits the rapid monitoring of thousands of cells under a given experimental condition, assessing their cellular integrity

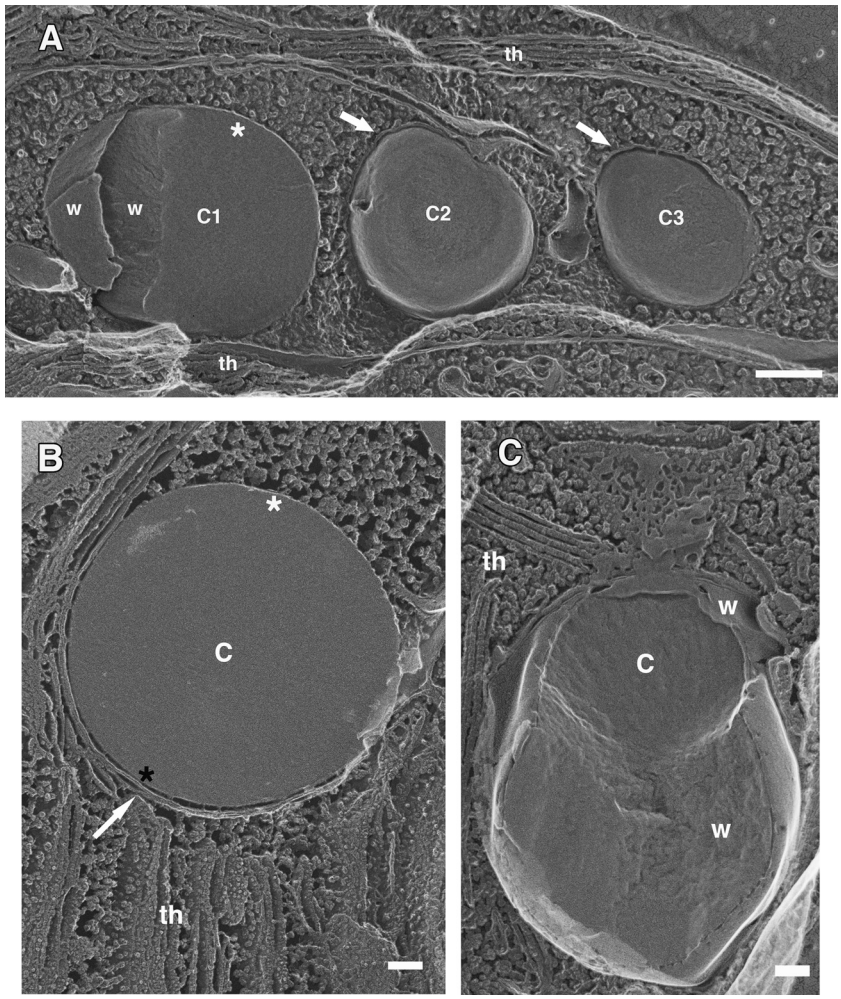

FIG. 11. Chloroplast LBs (additional images are presented in File 5 in the supplemental material). (A) Three cpst-LBs (C1 to C3). The asterisk marks the monolayer surrounding the rightward face of C1; arrows point to cross-fractured thylakoid wraps associated with C2 and C3. w, en face fractured thylakoid wraps associated with C1; th, thylakoids. *sta6* cells were N starved for 40 h. Bar, 250 nm. (B) Cpst-LB (C). The white asterisk marks its monolayer surface; the arrow indicates a thylakoid wrap, where a wrap bilayer is visible (black asterisk). th, thylakoids replete with IMPs. *sta6* cells were N starved for 15 h. Bar, 100 nm. (C) Cpst-LB (C) with en face views of IMP-free thylakoid wraps (w) flowing over the LB surface. th, thylakoids. *sta6* cells were N starved for 40 h. Bar, 100 nm. Degenerating thylakoids are visible at the top of field.

and size, their LB content and size, and the extent to which LBs fill cellular volumes.

The light micrographs in Fig. 1 and 2 illustrate a feature of LB content noted in our previous report (49), namely, an unexplained range in LB number and LB area per cell in a given culture during the first 2 days of N starvation. Interestingly, a similar range is encountered in differentiating adipocytes in culture (25). When N starvation was continued beyond 2 days, the per-cell variation persisted (Fig. 3 to 5) even as the LBs became much larger.

Since LB area does not accurately translate into volume as LB size increases, LB area was not quantitated in this study, but four features of LB biogenesis were revealed by counting total LBs per cell regardless of their size (Fig. 6). First, *sta6* cells had 1.5 to 2 times as many LBs as *STA6* cells at all stages of induction, presumably reflecting their production of both β-cyto-LBs and cpst-LBs. Second, the range of numbers of LBs/cell after the first 2 days of N starvation was much greater in the *sta6* strain than in the *STA6* strain, suggesting that control of LB number is more stringent for β-cyto-LBs than for cpst-LBs. Third, the general overall similarity in numbers of LBs/cell with time for a given strain indicates that LBs do not increase in size during induction by fusing with one another. And fourth, the increase in TAGs/cell with N starvation was not accomplished by the *de novo* synthesis of more LBs but rather by the progressive filling of existing LBs.

Conditions conducive to LB formation. We found that N-stress-induced LB formation is acetate dependent in the *STA6* and *sta6* strains (Fig. 2C), as reported for the *STA6* strain using TAG quantitation (9). In contrast, Li et al. (24) reported robust TAG production in the *sta6* strain in the absence of acetate. A possible explanation for this discrepancy (24) is that the cells were exposed to 10-fold-higher light intensities in addition to N starvation, which may enhance photosynthetic contributions and/or induce additional stress. A distantly related species, *C. monoica*, is an obligate phototroph, incapable of exogenous acetate utiliza-

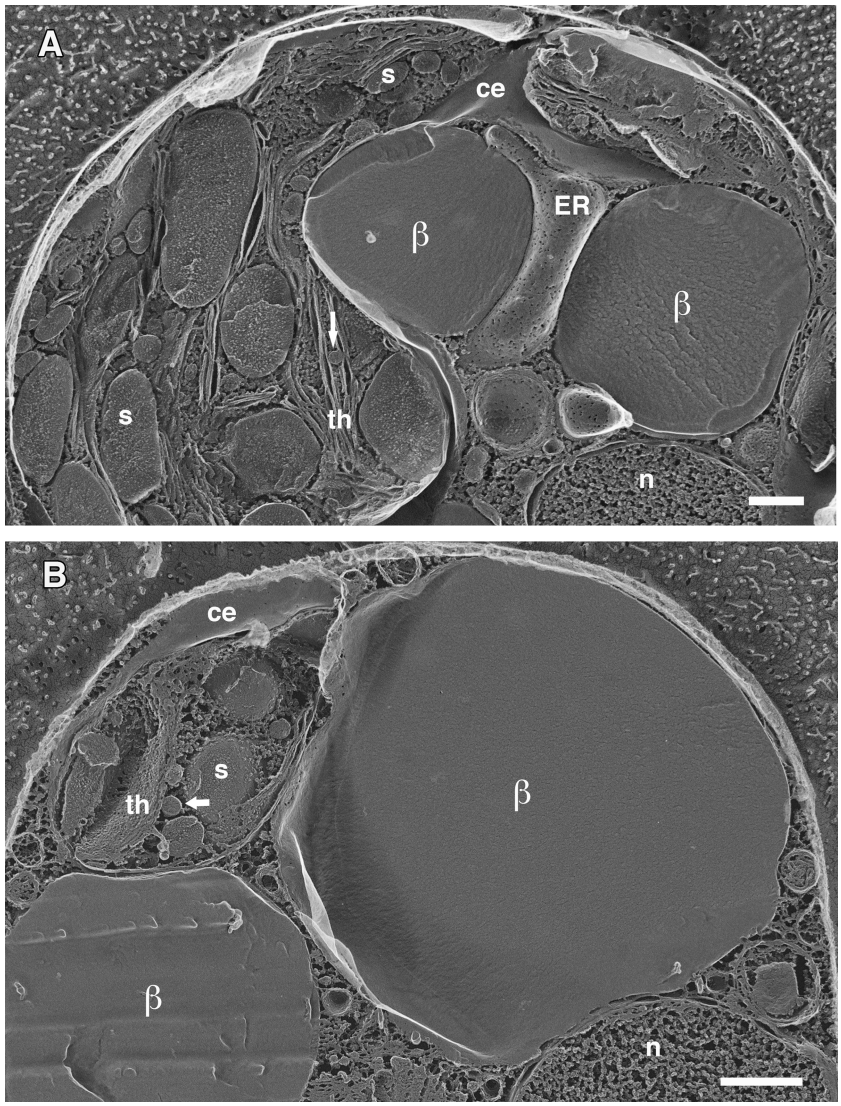

FIG. 12. Extended N starvation and acetate boost of *STA6* cells (additional images are presented in File 5 in the supplemental material). (A) A *STA6* cell that was N starved for 4 days with an acetate boost. The chloroplast is replete with starch (s) and contains extended thylakoids (th) and a plastoglobule (arrow). ce, OMCE; n, nucleus. Bar, 500 nm. (B) *STA6* cell that was N starved for 14 days with an acetate boost. Reduced chloroplast domain contains some thylakoid stacks (th), limited starch (s), and a plastoglobule (arrow). n, nucleus. Bar, 500 nm. Canonical β-cyto-LB interactions with the ER and nuclear envelope and OMCE (ce) can be seen in both panels.

tion, yet it produces abundant LBs after N starvation in low light (26, 38; K. VanWinkle-Swift and U. Goodenough, unpublished data). Hence the acetate requirement trait is clearly plastic and putatively amenable to genetic and/or environmental manipulation.

When acetate is present and log-phase *STA6* or *sta6* cells are N starved in the dark, LB production is compromised (9, 24). The contribution of photosynthesis to final LB yield in *C. reinhardtii* may not be extensive, given reported decreases in CO_2 fixation rates (28), RuBisCO and cpst-ATP synthase levels (35), chlorophyll levels (44, 51), thylakoid integrity (28, 31; also this study), and photosynthetic electron transport (6, 24, 51) during the course of N starvation. That said, the dark inhibition indicates that a feature(s) of photosynthesis, and/or perhaps an additional light-sensitive pathway(s), may be important to at least the early phases of LB production.

During the course of N starvation in *C. reinhardtii*, cells undergo extensive autophagy, influenced by the target-of-rapamycin (TOR) pathway (36), that initially involves the destruction of ribosomes (27, 28) and then the dismantling of other organelles, notably the chloroplast thylakoids (this study), until each LB-engorged obese cell is reduced to a minimal set of organelles, a chloroplast envelope, and a nucleus (Fig. 12 to 14). We are currently collaborating with investigators who employ solid-state nuclear magnetic resonance (NMR) methods to ascertain the extent to which LB biogenesis utilizes carbon skeletons derived from photosynthesis versus exogenous acetate versus products of autophagy. In one

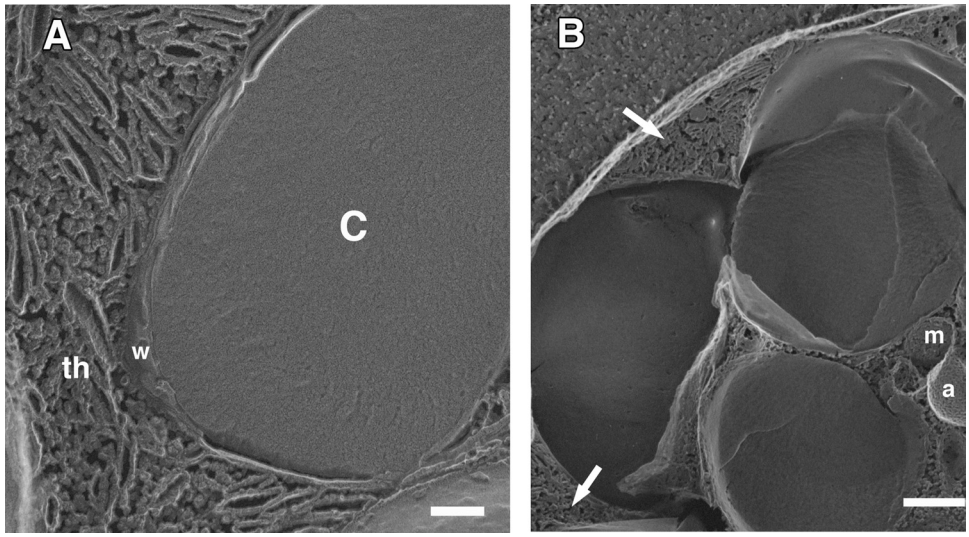

FIG. 13. Extended N starvation and acetate boost of *sta6* cells (additional images are presented in File 5 of the supplemental material). (A) *sta6* cell that was N starved for 4 days with an acetate boost. Thylakoids (th) are severed into short segments. c, cpst-LB; w, thylakoid wrap. Bar, 100 nm. (B) *sta6* cell that was N starved for 10 days with an acetate boost. Small chloroplast regions (arrows) contain severed thylakoids. a, acidocalcisome; m, mitochondrion. Bar, 500 nm.

scenario, autophagy may supply substrates to maintain cell viability while exogenous acetate feeds into LB production; in other scenarios, these tasks may be more evenly distributed.

Importantly, while exogenous acetate is necessary for the production of β- and cpst-LBs under the conditions we employed, acetate is not necessary for the production of *C. reinhardtii* biomass; the LB output of cells grown phototrophically in minimal salt medium and then N starved in the presence of acetate was comparable to that of cells grown mixotrophically (Fig. 2E; also, see File 3 in the supplemental material). Hence, the energy and carbon needed to generate *C. reinhardtii* cellular biomass can be derived exclusively from photosynthetic electron transport and CO_2 fixation, an important consideration should this species be considered as a production strain for biodiesel.

Cytoplasmic LBs. LBs are often regarded as organelles associated with lipid storage in specialized tissues (e.g., adipocytes and seeds); however, as detailed in reviews (10, 29, 33, 47), LBs are in fact ubiquitous and dynamic eukaryotic cellular components that feature in various aspects of intracellular lipid trafficking. In the *C. reinhardtii* cytoplasm, the small α-cyto-LBs (Fig. 7C and D) are apparent examples of such "constitutive"

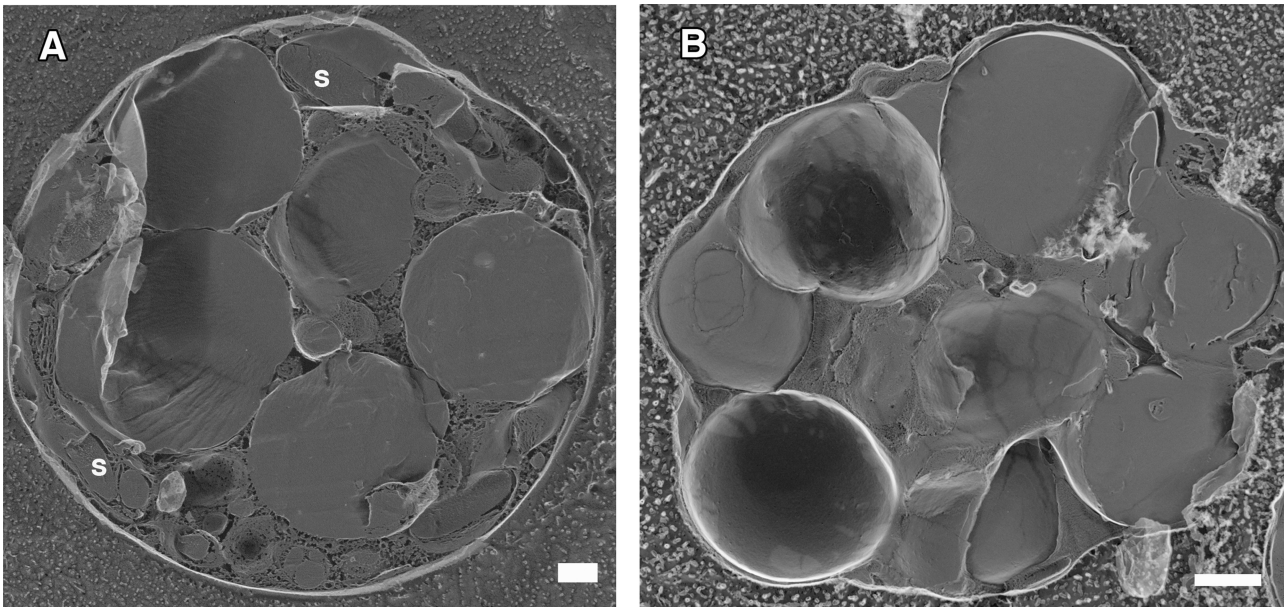

FIG. 14. Comparison of obese *STA6* cells after 14 days of N starvation with an acetate boost (A) and *sta6* cells after 7 days of N starvation with an acetate boost (B). The *STA6* cells retain more cytoplasm even after an additional week of N starvation. s, starch. Bars, 500 nm.

organelles: they are encountered at low levels in cycling cells, they are restricted to a narrow size range, and they exist either as apparently single entities or in contact with the ER or other organelle membranes, possibly thereby receiving signals and/or substrates for expansion or breakdown. The small constitutive plastoglobules (Fig. 7B and 12A and B) may play analogous roles in lipid trafficking in the *C. reinhardtii* chloroplast.

When subjected to N stress, the *C. reinhardtii* cytoplasm developed β-cyto-LBs that enlarge until, with an acetate boost, they eventually occupy most of the cytoplasmic volume (Fig. 3 to 5 and 12 to 14). In our previous study (49), the β-cyto-LBs from the *STA6* strain and the *sta6* strain were purified and analyzed biochemically (the purification protocol excluded cpst-LBs) and were found to have very similar fatty acid profiles.

The ER is well established as the primary locus of glycerol-3-P esterification to form diacylglycerides (DAGs) and TAGs (3); in land plants, the ER localization of diacylglycerol acyltransferase (DAGAT) and phospholipid:diacylglycerolacyltransferase (PDAT), which catalyze TAG synthesis, is under tight regulation (12). We observed a close association between one face of each β-cyto-LB and an ER cisterna, where continuities between the outer leaflet of the ER bilayer and the delimiting cyto-LB monolayer could be resolved (Fig. 8B). Unexpectedly, the opposite face of each β-cyto-LB was associated with the outer membrane of the chloroplast envelope (OMCE) (Fig. 8 to 10 and 12A and B), with membrane continuities also readily resolved. These observations suggest that both the ER membrane and the OMCE participate in β-cyto-LB biogenesis in *C. reinhardtii*.

In green organisms, fatty acids are synthesized in the chloroplast and are then somehow shuttled to the ER for esterification to glycerol backbones (3, 9, 19). Evidence has recently been obtained in land plants for ER domains called PLAMs (plastid-associated membranes) that represent stable associations between the ER and the outer chloroplast envelope (1, 48, 52). We have not identified stable PLAM configurations in log- or stationary-phase *C. reinhardtii*, but they may exist transiently, allowing chloroplast-derived acyl coenzyme A to interact with ER enzymes to generate polar lipids without an intervening transit through the cytoplasm.

Such configurations, in contrast, are highly stable in N-starved cells, the result being TAG-filled β-cyto-LBs enclosed in a monolayer of polar lipids apparently provided by the outer leaflets of both the OMCE and ER membranes. A model depicting these relationships is shown in Fig. 15. The monolayer lipids may occupy segregated domains as depicted in Fig. 15 or, more likely, may diffuse in the plane of the half-membrane to form a hybrid mixture. Recent data from Fan et al. (9) indicate that such a route may be traversed by chloroplast-derived DAG as well as by free fatty acids.

Two biochemical observations support this model. We showed previously (49) that the two prominent polar lipids associated with purified β-cyto-LBs in *C. reinhardtii* are 1,2-diacylglyceryl-3-*O*-4-(*N*,*N*,*N*-trimethylhomoserine) (DGTS), unique to ER membranes (3), and sulfoquinovosyldiacylglycerol (SQDG), unique to chloroplast membranes (3), suggesting that both organelles contribute polar lipids to the enclosing β-cyto-LB monolayer. We also found that ~10% of the lipid in purified β-cyto-LBs takes the form of free fatty acids.

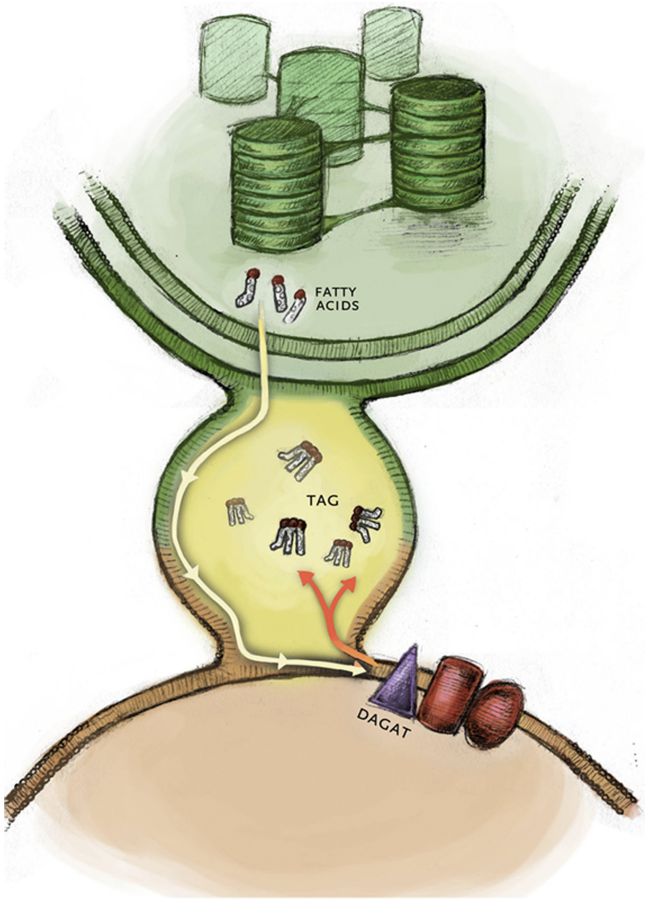

FIG. 15. Proposed relationship between ER and chloroplast during β-cyto-LB formation. Fatty acids synthesized in the chloroplast stroma, and perhaps also DAG (9), diffuse along the LB-delimiting monolayer created jointly by the OMCE and ER; when they reach diacylglycerol acetyltransferases (DAGAT) in the ER membrane, they are esterified to glycerol to form TAG, which then enters the LB interior.

The morphological studies presented here are best interpreted as indicating that under conditions of N stress, α-cyto-LBs establish stable ER-OMCE relationships and enlarge to form β-cyto-LBs, as contrasted with the alternative possibility that β-cyto-LBs form *de novo*.

Chloroplast LBs. Cpst-LB formation in the *sta6* strain is prominent during the 12- to 24-h period following N starvation from log phase, a period of intensive starch accumulation in wt strains (27, 32, 41, 51), consistent with the hypothesis that the block in starch biosynthesis allows substrates and/or ATP/NADPH to shuttle into cpst-LB production. In our confocal microscopic assays (49), *sta6* cells were calculated to contain three times the total LB volume of *STA6* cells after a 2-day N starvation from stationary phase; enhanced TAG synthesis by the *sta6* strain has also been reported by others (23, 51). While Siaut et al. (44) documented a variability in the numbers of TAGs/cell of various *C. reinhardtii* strains under various induction conditions, the microscopic data presented here demonstrate that under the conditions we employed, the *sta6* strain accumulates more (Fig. 6), and larger, LBs than the *STA6* strain until late in the acetate boost regimen, at which time the

STA6 strain has consumed most of its starch reserves and appears to catch up (Fig. 5 and 14).

To date, cpst-LBs have been observed only in the *sta6* strain; we have not observed any cpst-LBs in starch-producing strains under a variety of conditions or in three *sta6* strains complemented with *STA6* transgenes. Recently, Fan et al. (9) published thin-section images showing *sta6* cpst-LBs. They did not, however, examine images of starch-producing cells and hence failed to recognize that cpst-LBs do not form in wt *C. reinhardtii* under the induction conditions that they, and we, employed.

In *STA6* and *sta6* cells, the chloroplasts contain small plastoglobules (Fig. 7B and 12A and B) that are presumably homologous to the plastoglobules detected in other algae (20, 22) and land plants (5, 18), where they are reported to contain TAG (17). The chloroplasts also contain carotenoid-rich eyespot granules (Fig. 7A) that contain TAG (31). Hence it seems likely, although it has not yet been demonstrated experimentally, that the *C. reinhardtii* chloroplast contains enzymes that catalyze TAG biosynthesis in N-replete cells.

One possible explanation for the *sta6* cpst-LB phenotype, therefore, is that substrates, reductants, and ATP normally directed to starch biosynthesis are diverted to a constitutive cpst-TAG-biosynthetic pathway under N-stress conditions. An alternative explanation is that the *C. reinhardtii* genome includes information for an inducible cpst-TAG-biosynthetic pathway that is expressed under N-stress conditions when starch biosynthesis is blocked (and possibly under other conditions as well). The finding that *C. reinhardtii* possesses two TAG-biosynthetic pathways, one of which is exposed or stimulated in the presence of a single gene mutation, expands opportunities for genetic and/or environmental manipulation of the LB trait in this species, and possibly in other algae as well.

Morphologically, the *sta6* cpst-LBs are very different from plastoglobules, growing to >1 μm in diameter and commonly wrapped with thylakoid membranes rather than making punctate thylakoid contact. As noted above for β-cyto-LBs, no DEEM images have been encountered that could be interpreted as showing small incipient cpst-LBs, consistent with the possibility that plastoglobules may serve as "seeds" for cpst-LBs. That said, the plastoglobule population of *sta6* cells remains stable throughout cpst-LB production, as does the cpst-LB population (Fig. 6), so presumably only a subpopulation of plastoglobules would serve as such seeds. Thylakoids in apparent states of disassembly are also often encountered in proximity to cp-LBs (Fig. 11C), consistent with the possibility that their breakdown (via lipase or PDAT activity) may contribute to cpst-LB TAG synthesis. And presumably, the bulk of cpst-LB TAG biosynthesis takes advantage of pathways and substrates that otherwise would have participated in starch biosynthesis.

Each cpst-LB is surrounded by a lipid monolayer, and each is also partially or totally wrapped by one or more IMP-free thylakoids. The images suggest that cpst-LB monolayers derive from thylakoid wrap bilayers in a fashion similar to the derivation of β-cyto-LB monolayers from ER and OMCE bilayers. The structural complexity of this system is concordant with the thesis that cpst-LB formation in *C. reinhardtii* is an encoded trait and not simply the consequence of aberrations generated by the *sta6* mutation.

Extended induction and the acetate boost. In our prior study using stationary-phase *STA6* and *sta6* cells (49), cell viability became compromised after 2 days of N starvation. In contrast, cells remain viable up to 4 days when N starved from log phase, the protocol employed in this study and also in other published studies of the *C. reinhardtii* LB system (9, 21, 23, 24, 30, 31, 44, 51).

Siaut et al. (44) documented a linear increase in number of TAGs/cell in the *STA6* strain during days 1 to 5 after N starvation from log phase, followed by a plateau; we found that the *STA6* and *sta6* strains become moribund after 4 days even when induced from log phase. If, however, either strain was given a 20 mM acetate boost after 2 days of N starvation, the cells remained viable for up to 2 weeks, and the sizes of both β-cyto-LBs and, in the *sta6* strain, cpst-LBs increased dramatically until the cells became fully engorged, or obese (Fig. 3 to 5 and 12 to 14). Obese *STA6* cells are hardier and die later than the *sta6* cells, possibly because they only slowly deplete their starch reserves and retain normal-looking thylakoids. Neither *STA6* nor *sta6* cells changed in size while becoming obese, because their cytoplasmic contents, most prominently their large chloroplasts, undergo autophagy as the LBs enlarge.

Given that *C. reinhardtii* cells can be induced to fill virtually their entire volume with LBs, further augmentation of acetate-promoted TAG yield with this species is most likely to be achieved by either increasing cell size or increasing cell number/ml.

By 7 days after N starvation with an acetate boost, obese *sta6* cells floated and failed to pellet with centrifugation at 100,000 × *g*. This was not the case for obese *STA6* cells even after 14 days, presumably because they continued to contain starch (Fig. 4, 5, 12, and 14), which is very dense (46). The *sta6* flotation property may have applications in cell harvesting, a key challenge in developing algae for biofuel production.

ACKNOWLEDGMENTS

This work was supported by a grant to the NAABB Consortium from the U.S. Department of Energy and by the International Center for Advanced Renewable Energy and Sustainability (I-CARES) at Washington University.

We thank Jeremy King and John Heuser for pilot experiments, Steven Ball and David Dauvillée for complemented *sta6* strains, and Jae-Hyeok Lee for zygotes. Figure 6 was prepared by Janette Kropat, and Fig. 15 was drawn by Mara MacMahon.

REFERENCES

1. **Andersson, M. X., M. Goksor, and A. M. Sandelius.** 2007. Optical manipulation reveals strong attracting forces at membrane contact sites between endoplasmic reticulum and chloroplasts. J. Biol. Chem. **282:**1170–1174.
2. **Austin, J. R., II, E. Frost, P.-A. Vidi, F. Kessler, and L. A. Staehelin.** 2006. Plastoglobules are lipoprotein subcompartments of the chloroplast that are permanently coupled to thylakoid membranes and contain biosynthetic enzymes. Plant Cell **18:**1693–1703.
3. **Benning, C.** 2009. Mechanisms of lipid transport involved in organelle biogenesis in plant cells. Annu. Rev. Cell Dev. Biol. **25:**71–91.
4. **Bourguignon, L. Y. W., and G. E. Palade.** 1976. Incorporation of polypeptides into thylakoid membranes of *Chlamydomonas reinhardtii*. J. Cell Biol. **69:**327–344.
5. **Bréhélin, C., F. Kessler, and K. J. van Wijk.** 2007. Plastoglobules: versatile lipoprotein particles in plastids. Trends Plant Sci. **12:**260–266.
6. **Bulté, L., and F-A. Wollman.** 1992. Evidence for a selective destabilization of an integral membrane protein, the cytochrome b_6/f complex, during gametogenesis in *Chlamydomonas reinhardtii*. Eur. J. Biochem. **204:**327–336.
7. **De Petrocellis, B., P. Siekevitz, and G. E. Palade.** 1970. Changes in chemical composition of thylakoid membranes during greening of the *y-1* mutant of *Chlamydomonas reinhardi*. J. Cell Biol. **44:**618–634.
8. **Docampo, R., P. Ulrich, and S. N. J. Moreno.** 2010. Evolution of acidocalcisomes and their role in polyphosphate storage and osmoregulation in eukaryotic microbes. Philos. Trans. R. Soc. B **365:**775–784.
9. **Fan, J., C. Andre, and C. Xu.** 2011. A chloroplast pathway for the de novo biosynthesis of triacylglycerol in *Chlamydomonas reinhardtii*. FEBS Lett. **585:**1985–1991.

10. **Farese, R. V., and T. C. Walther.** 2009. Lipid droplets finally get a little R-E-S-P-E-C-T. Cell **139:**855–860.
11. **Fujimoto, T., Y. Ohsaki, J. Cheng, M. Suzuki, and Y. Shinohara.** 2008. Lipid droplets: a classic organelle with new outfits. Histochem. Cell Biol. **130:**263–279.
12. **Gidda, S. K., et al.** 2011. Hydrophobic-domain-dependent protein-protein interactions mediate the localization of GPAT enzymes to ER subdomains. Traffic **12:**452–472.
13. **Gorman, D. S., and R. P. Levine.** 1965. Cytochrome *f* and plastocyanin: their sequence in the photosynthetic electron transport chain of *Chlamydomonas*. Proc. Natl. Acad. Sci. U. S. A. **54:**1665–1669.
14. **Harris, E. H.** 2009. The Chlamydomonas sourcebook. I. Introduction to Chlamydomonas and its laboratory use. Elsevier, Amsterdam, The Netherlands.
15. **Heuser, J. E.** 2011. The origins and evolution of freeze-etch electron microscopy. J. Electron Microsc. **60:**S3–S29.
16. **Hu, Q., et al.** 2008. Microalgal triacylglycerols as feedstocks for biofuel production: perspectives and advances. Plant J. **54:**621–639.
17. **Kaup, M. T., C. D. Froese, and J. E. Thompson.** 2002. A role for diacylglycerol acyltransferase during leaf senescence. Plant Physiol. **129:**1616–1628.
18. **Kessler, F., and P.-A. Vidi.** 2007. Plastoglobule lipid bodies: their functions in chloroplasts and their potential for applications. Adv. Biochem. Eng. Biotechnol. **107:**153–172.
19. **Koo, A. J. K., J. B. Ohlrogge, and M. Pollard.** 2004. On the export of fatty acids from the chloroplast. J. Biol. Chem. **279:**16101–16110.
20. **Kreimer, G.** 2009. The green algal eyespot apparatus: a primordial visual system and more? Curr. Genet. **55:**19–43.
21. **Kropat, J., et al.** 2011. A revised mineral nutrient supplement increases biomass and growth rate in *Chlamydomonas reinhardtii*. Plant J. **66:**770–780.
22. **Lamars, P. P., et al.** 2010. Carotenoid and fatty acid metabolism in light-stressed *Dunaliella salina*. Biotech. Bioeng. **106:**638–648.
23. **Li, Y., et al.** 2010a. *Chlamydomonas* starchless mutant defective in ADP-glucose pyrophosphorylase hyper-accumulates triacylglycerol. Metab. Eng. **12:**387–391.
24. **Li, Y., D. Ham, G. Hu, M. Sommerfeld, and Q. Hu.** 2010b. Inhibition of starch synthesis results in overproduction of lipids in *Chlamydomonas reinhardtii*. Biotechnol. Bioeng. **107:**258–268.
25. **Loo, L.-H., et al.** 2009. Heterogeneity in the physiological states and pharmacological responses of differentiating 3T3-L1 preadipocytes. J. Cell Biol. **187:**375–384.
26. **Malmberg, A. E., and K. P. VanWinkle-Swift.** 2001. Zygospore germination in *Chlamydomonas monoica* (Chlorophyta): timing and pattern of secondary zygospore wall degradation in relation to cytoplasmic events. J. Phycol. **37:**86–94.
27. **Martin, N. C., and U. W. Goodenough.** 1975. Gametic differentiation in *Chlamydomonas reinhardi*. I. Production of gametes and their fine structure. J. Cell Biol. **67:**587–605.
28. **Martin, N. C., K. S. Chiang, and U. W. Goodenough.** 1976. Turnover of chloroplast and cytoplasmic ribosomes during gametogenesis in Chlamydomonas reinhardi. Dev. Biol. **51:**190–201.
29. **Martin, S., and R. G. Parton.** 2006. Lipid droplets: a unified view of a dynamic organelle. Nat. Rev. Mol. Cell. Biol. **7:**373–377.
30. **Miller, R., et al.** 2010. Changes in transcript abundance in *Chlamydomonas reinhardtii* following nitrogen deprivation predict diversion of metabolism. Plant Physiol. **154:**1737–1752.
31. **Moellering, E. R., and C. Benning.** 2010. RNA interference silencing of a major lipid droplet protein affecting lipid droplet size in *Chlamydomonas* reinhardtii. Eukaryot. Cell **9:**97–106.
32. **Mouille, G., et al.** 1996. Preamylopectin processing: a mandatory step for starch biosynthesis in plants. Plant Cell **8:**1353–1366.
33. **Murphy, D. J.** 2001. The biogenesis and functions of lipid bodies in animals, plants, and microorganisms. Prog. Lipid Res. **40:**325–438.
34. **Ohad, I., P. Siekevitz, and G. E. Palade.** 1967. Biogenesis of chloroplast membranes. I. Plastid dedifferentiation in a dark-grown algal mutant (*Chlamydomonas reinhardi*). J. Cell Biol. **35:**521–552.
35. **Park, H., L. L. Eggink, R. W. Roberson, and J. K. Hoober.** 1999. Transfer of proteins from the chloroplast to vacuoles in *Chlamydomonas reinhardtii* (Chlorophyta): a pathway for degradation. J. Phycol. **35:**528–538.
36. **Pérez-Pérez, M. E., F. J. Florencio, and J. L. Crespo.** 2010. Inhibition of target of rapamycin signaling and stress activate autophagy in *Chlamydomonas* reinhardtii. Plant Physiol. **152:**1874–1888.
37. **Radakovits, R., R. E. Jinkerson, A. Darzins, and M. C. Posewitz.** 2010. Genetic engineering of algae for enhanced biofuel production. Eukaryot. Cell **9:**486–501.
38. **Rickoll, W., D. Rehkopf, C. Dunn, A. Malmberg, and K. VanWinkle-Swift.** 1998. The *sta-1* mutation prevents assembly of starch granules in nitrogen-starved cells and serves as a useful morphological marker during sexual reproduction in *Chlamydomonas monoica* (Chlorophyceae). J. Phycol. **34:**147–151.
39. **Ruiz, F. A., N. Marchesini, M. Seufferheld, Govindjee, and R. Docampo.** 2001. The polyphosphate bodies of *Chlamydomonas reinhardtii* possess a proton-pumping pyrophosphatase and are similar to acidocalcisomes. J. Biol. Chem. **276:**46196–46203.
40. **Sager, R., and G. E. Palade.** 1957. Structure and development of the chloroplast in Chlamydomonas. I. The normal green cell. J. Biophys. Biochem. Cytol. **3:**463–488.
41. **Schmidt, M., et al.** 2006. Proteomic analysis of the eyespot of Chlamydomonas reinhardtii provides novel insights into its components and tactic movements. Plant Cell **18:**1908–1930.
42. **Schmidt, M. A., and E. M. Herman.** 2008. Suppression of soybean oleosin produces micro-oil bodies that aggregate into oil body/ER complexes. Mol. Plant **1:**910–924.
43. **Scott, S. A., et al.** 2010. Biodiesel from algae: challenges and prospects. Curr. Opin. Biotechnol. **21:**277–286.
44. **Siaut, M., et al.** 2011. Oil accumulation in the model green alga *Chlamydomonas reinhardtii:* characterization, variability between common laboratory strains and relationship with starch reserves. BMC Biotechnology **11:** 7–22.
45. **Sueoka, N.** 1960. Mitotic replication of deoxyribonucleic acid in Chlamydomonas reinhardi. Proc. Natl. Acad. Sci. U. S. A. **46:**83–91.
46. **Sujka, M., and J. Jamroz.** 2007. Starch granule porosity and its changes by means of amylolysis. Int. Agrophysics **21:**107–113.
47. **Thiele, C., and J. Spandi.** 2008. Cell biology of lipid droplets. Curr. Opin. Cell Biol. **20:**378–386.
48. **Tomova, C., et al.** 2009. Membrane contact sites between apicoplast and ER in *Toxoplasma gondii* revealed by electron tomography. Traffic **10:**1471–1480.
49. **Wang, Z. T., N. Ullrich, S. Joo, S. Waffenschmidt, and U. Goodenough.** 2009. Algal lipid bodies: stress induction, purification, and biochemical characterization in wild-type and starchless *Chlamydomonas reinhardtii*. Eukaryot. Cell **8:**1856–1868.
50. **Wijffels, R. H., and M. J. Barbosa.** 2010. An outlook on microalgal biofuels. Science **329:**796–799.
51. **Work, V. H., et al.** 2010. Increased lipid accumulation in the *Chlamydomonas reinhardtii sta7-10* starchless isoamylase mutant and increased carbohydrate synthesis in complemented strains. Eukaryot. Cell **9:**1251–1261.
52. **Xu, C., J. Fan, A. J. Cornish, and C. Benning.** 2008. Lipid trafficking between the endoplasmic reticulum and plastid in *Arabidopsis* requires the extraplastidic TGD4 protein. Plant Cell **20:**2190–2204.
53. **Zabawinski, C., et al.** 2001. Starchless mutants of *Chlamydomonas reinhardtii* lack the small subunit of a heterotetrameric ADP-glucose pyrophosphorylase. J. Bacteriol. **183:**1069–1077.